Simulating the behavior of prestressed beams with different degrees of prestressing

Marino Jurišić
University of Mostar, Faculty of Civil Engineering, M.Eng.C.E.
marino.jurisic@gf.sum.ba
Dragan Ćubela
University of Mostar, Faculty of Civil Engineering, Ph.D C.E.
dragan.cubela@gf.sum.ba
Mladen Kustura
University of Mostar, Faculty of Civil Engineering, Ph.D C.E.
mladen.kustura@gf.sum.ba

Abstract: The paper covers numerical analysis of an experiment with five T-beams that are loaded to failure. The beams are designed to have the same ultimate bearing capacity with different ratios of prestressed to classic reinforcement. A detailed overview of the experiment is shown with exact section dimensions, as well as exact position and ratio of prestressed to classic steel. As a result of the experiment, force-displacement diagrams for each beam are presented and analyzed. Numerical model of the beams, reinforced in accordance with the experiment, is also shown. Two models for materials are used to analyze the beams: design model to check the design failure force and a new material model with concrete tension to simulate the actual behavior of the beams. All beams are gradually loaded to numerical failure by incrementally increasing the load that simulates press load. At the end, an analysis and comparison between experimental and numerical results is conducted to determine if the numerical model is a good representation of actual beam behavior.

Key words: experiment, prestressing, numerical model, material model, nonlinear analysis

Simuliranje ponašanja prednapetih nosača sa različitim stupnjem prednapinjanja

Sažetak: U radu numerički se obrađuje eksperiment u kojem je napravljeno 5 „T" nosača koji su opterećeni do loma pod presom. Nosači su projektirani tako da imaju istu graničnu nosivost uz različit odnos armiranja prednapetom i mekom armaturom. Daje se detaljan pregled eksperimenta sa točnim dimenzijama presjeka, kao i točnim položajem i odnosom prednapete i meke armature. Kao rezultat eksperimenta prikazane su i analizirane krivulje sila-pomak na pojedinim nosačima. Prikazan je i numerički model za nosače armirane prema eksperimentu. Korištena su dva modela materijala za analizu nosača; računski model materijala kako bi se provjerila računska lomna sila nosača i novi proizvoljni model materijala u kojem se određuje posebno ponašanje betona u vlaku kako bi se simuliralo stvarno ponašanje nosača. Svi nosači su postupno dovedeni do numeričkog loma inkrementalnim povećavanjem opterećenja koje simulira povećanje opterećenja na presi. Naposljetku, daje se analiza i usporedba rezultata numeričkog modela sa eksperimentom, kao i zaključak o valjanosti numeričkog modela.

Ključne riječi: eksperiment, prednapinjanje, numerički model, model materijala, nelinearna analiza

1.   OVERVIEW OF THE EXPERIMENT

The experiment was performed in cooperation with the Department of Structural Engineering, Faculty of Civil Engineering, University of Mostar, and the Department of Concrete Structures and Bridges, Faculty of Civil Engineering, Architecture and Geodesy, University of Split, as part of two doctoral theses. [1] [2] Five types of beams (A, B, C, D and E) were tested in the experiment, and the beam type C is treated here. The beam type C is a classic T section of a floor beam that is most commonly used as a ceiling or roof load-bearing element. These beams are one of the most rational and most used in practice. They can be made with prestressed and with classic reinforcement. Usual spans are 8 – 12 m. Beams with a total length of 10 m are made in this experiment. The type of static system is simple beam with a span of 9.5 m (beams hanging over supports 0.25 cm). In cross section, the width of the upper flange is 80 cm, while the width of the web is 40 cm. The total height of the section is 50 cm, the height of the upper flange is 15 cm, and of the flat part of the web is 32 cm. The lower part of the upper flange is tapered in height by 3 cm from the web joint with a thickness of 18 cm to the edge of 15 cm. The geometry of the beam is shown in Figure 1.
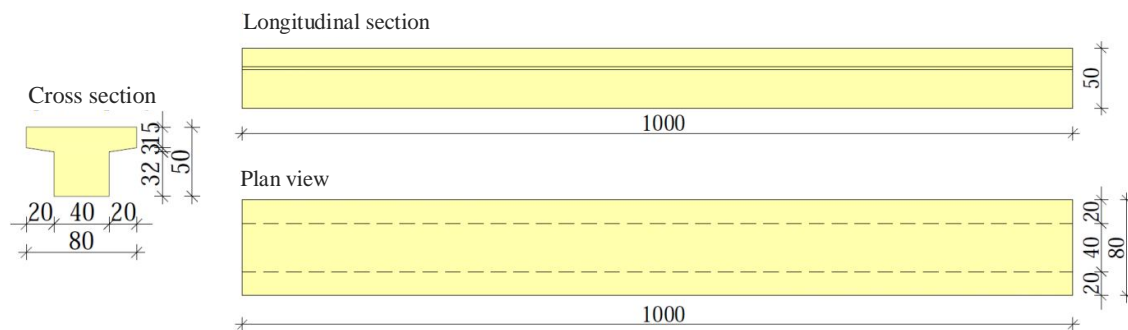

Figure 1. Geometry of the type C beam

Five type C beams were made, differing in the reinforcement of the lower zone, with different degrees of prestressing. The degree of prestressing is determined by the expression:

$$\mu_p = \frac{A_p}{A_p + n \cdot A_S}$$

Where:

μ_p – is the degree of prestressing
A_p – area of prestressed reinforcement
n – classic reinforcing steel to prestressing steel strength ratio
A_s – area of classic reinforcing steel

e-ZBORNIK   21/2021

Jurišić, M., Ćubela, D., Kustura, M.
Simulating the behavior of prestressed beams with different degrees of prestressing

The beams are designed to keep similar bearing capacity (the same mechanical reinforcement coefficient) but to have different degrees of prestressing. Thus, beam C1 is reinforced only with prestressed reinforcement and has the degree of prestressing $\mu_p = 1.0$. Beam C2 is reinforced mostly with prestressed reinforcement and in a small part with classic reinforcement and has the degree of prestressing $\mu_p = 0.8$. Beam C3 is reinforced roughly equally with prestressed and classic reinforcement with the degree of prestressing $\mu_p = 0.56$. Beam C4 is reinforced mostly with classic reinforcement and to a lesser extent with prestressed reinforcement with the degree of prestressing $\mu_p = 0.33$. Finally, beam C5 is reinforced only with classic reinforcement with the degree of prestressing $\mu_p = 0$.

All beams are made of concrete class C40/50. Classic deformed reinforcing bars with diameters from $\Phi 8mm$ to $\Phi 25mm$ made of B500B quality steel were used. In all beams, the prestressed reinforcement is tendons 3/8" in diameter woven from 7 wires (one central and 6 spiral ones) and with cross-sectional area of tendon 52 mm^2. The steel used for prestressed reinforcement is Y1860S7. The beams are prestressed using the technology of prestressing before hardening (pre-tensioned prestressing) on the prestressing bed. This technology involves prestressing of tendons before placing concrete, where the prestressing force is applied by anchors at the ends of the bed. After concrete is placed and hardened, the tendons are released from the anchors and the prestressing force is introduced into the concrete beam by friction between prestressing steel and concrete. Instantaneous losses due to wedge draw-in are negligible due to bed length, and instantaneous losses due to friction do not exist in this prestressing technology because friction is used to introduce force into the section. Of the instantaneous losses, only losses due to elastic shortening of the beam when applying the prestressing force are taken. The initial stress on the beam was σ_{p0} ≈ 1076.4 MPa. Table 1 shows the basic data on the reinforcement placed in the beams, the degree of prestressing μ_p and the initial prestressing force P_{m0}. Figure 2 shows the cross-sections of all subtypes of beams C (C1, C2, C3, C4, C5, as well as the basic reinforcement).

Table 1. Basic data on the reinforcement placed in the beams, the degree of prestressing μ_p and the initial prestressing force P_{m0}

Beam type	Prestressed reinforcement	Classic reinforcement	Degree of prestressing μ_p	Initial prestressing force P_{m0} (kN)
C1	10Φ3/8"	-	1.00	580
C2	8Φ3/8"	2Φ14	0.80	464
C3	5Φ3/8"	3Φ16	0.56	290
C4	3Φ3/8"	3Φ20	0.33	174
C5	-	1Φ22+2Φ25	0.00	-

a)   Basic reinforcement of the beam

Subtype C1

Subtype C2

Subtype C3

Subtype C4

Subtype C5

Figure 2. Reinforcement of tested concrete beams

Twelve samples were taken during concreting and the following were determined on them: compressive strength of concrete, flexural tensile strength of concrete and modulus of elasticity of concrete. Three samples are cubes with dimensions 150x150x150 mm. The cubes were stored in laboratory conditions and the compressive strength was tested on them after 28 days.

The other 9 samples were tested at the same time with the beam test. The compressive strength of concrete was tested on three cubes with dimensions 150x150x150 mm, the compressive strength and modulus of elasticity of concrete were tested on three cylinders with dimensions D/H = 150x300 mm, and the flexural tensile strength was tested on three prisms with dimensions 100x100x400 mm. The samples were stored under the same conditions as the beams until the time of testing.

Before placing reinforcement in the beams, samples of all profiles of reinforcement and prestressing tendons were taken from several batches and tested on a tensile testing machine, where the tensile strength and modulus of elasticity were determined. The parameters of concrete (Table 2) and parameters of classic (Table 3) and prestressed (Table 4) reinforcement for short-term loading are shown below.

Table 2. Parameters of concrete C40/50 for short-term loading

Concrete C40/50	
Density of concrete (t = 28 days)	ρ_c = 2444 kg/m^3
Compressive strength (t = 28 days) determined on cubes	f_{ck} = 56.8 MPa
Compressive strength (on the day of beam testing) determined on cubes	f_{ck} = 58.9 MPa
Compressive strength (on the day of beam testing) determined on cylinders	f_{ck} = 53.1 MPa
Compressive strength (after testing the beams) determined on cylinders taken from the beams	f_{ck} = 44.75 MPa
Tensile strength (on the day of beam testing) determined on prisms	f_{ct} = 7.4 MPa
Modulus of elasticity (on the day of beam testing) determined on cylinders	E_c = 36 GPa

Table 3. Parameters of reinforcing steel for short-term loading

Classic reinforcement B500B	
Modulus of elasticity	E_s = 205 GPa
Liquid limit	f_{yk} = 500 MPa
Strength	f_{yd} = 650 MPa

Table 4. Parameters of prestressed steel for short-term loading

Prestressed reinforcement Y1860S7	
Modulus of elasticity	E_p = 195 GPa
Liquid limit	f_{pk} = 1670 MPa
Strength	f_{pd} = 1900 MPa
Tendon diameter	9.5 mm (3/8 inch)
Tendon area	52 mm^2

After testing the beams, three cylinders were taken from the uncracked parts of the beam with a base diameter to height ratio of 1:2. The compressive strength of concrete was tested and the concrete stress-strain relationship in compression was experimentally determined on them. The average value of the results was taken as relevant. The uniaxial stress-strain diagrams for classic reinforcement (Figure 3), prestressed steel (Figure 4) and concrete in compression (Figure 5) are shown below. These diagrams will be used to adopt the material model in the numerical model (only the diagram for class C40/50 is used for concrete).
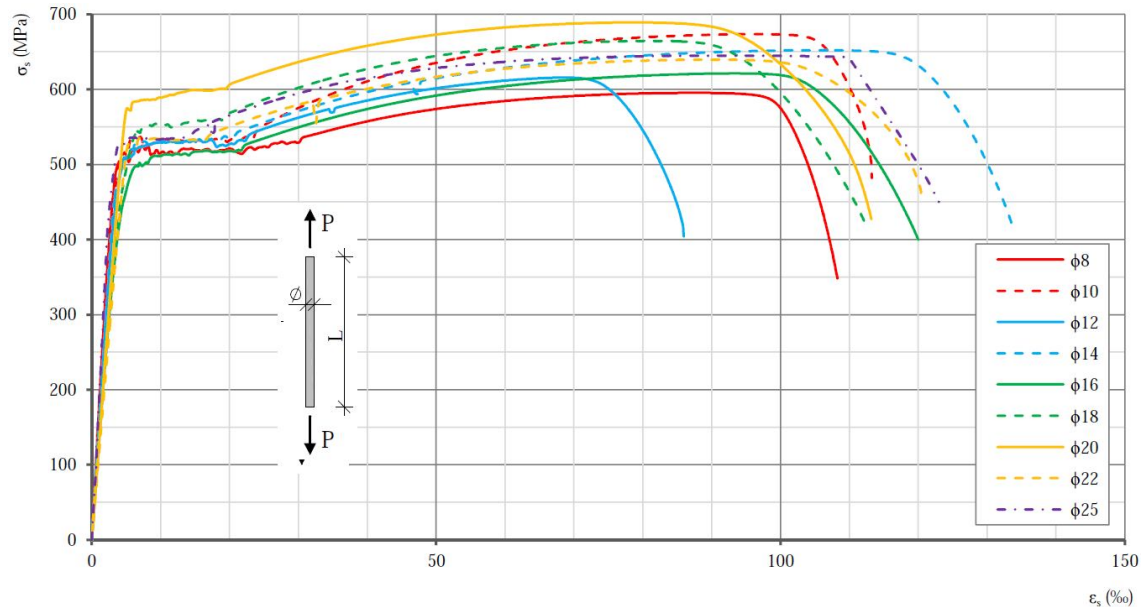
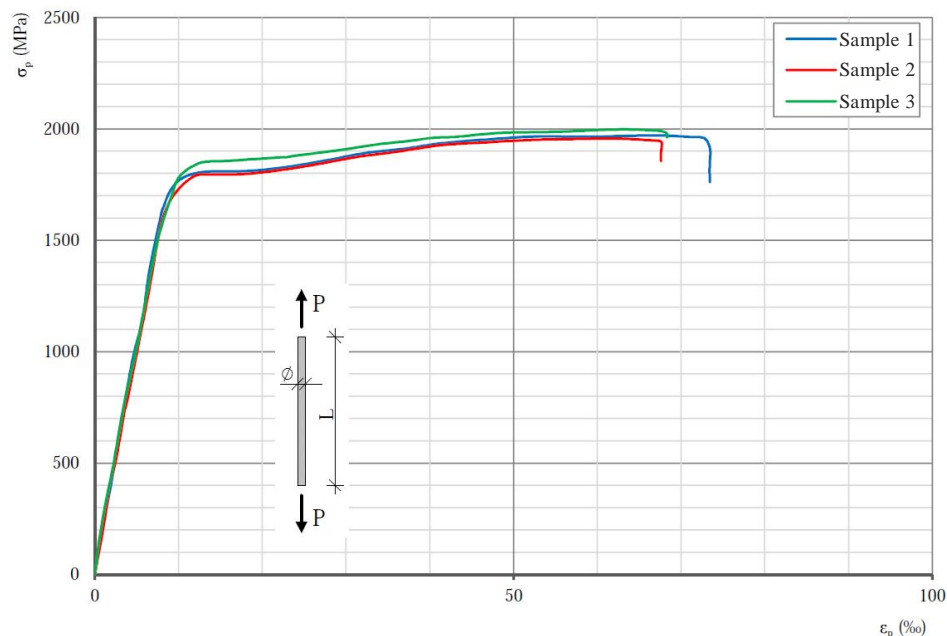Figure 3. Average values of the measured σ_s-ε_s relationship for concrete steel B500B

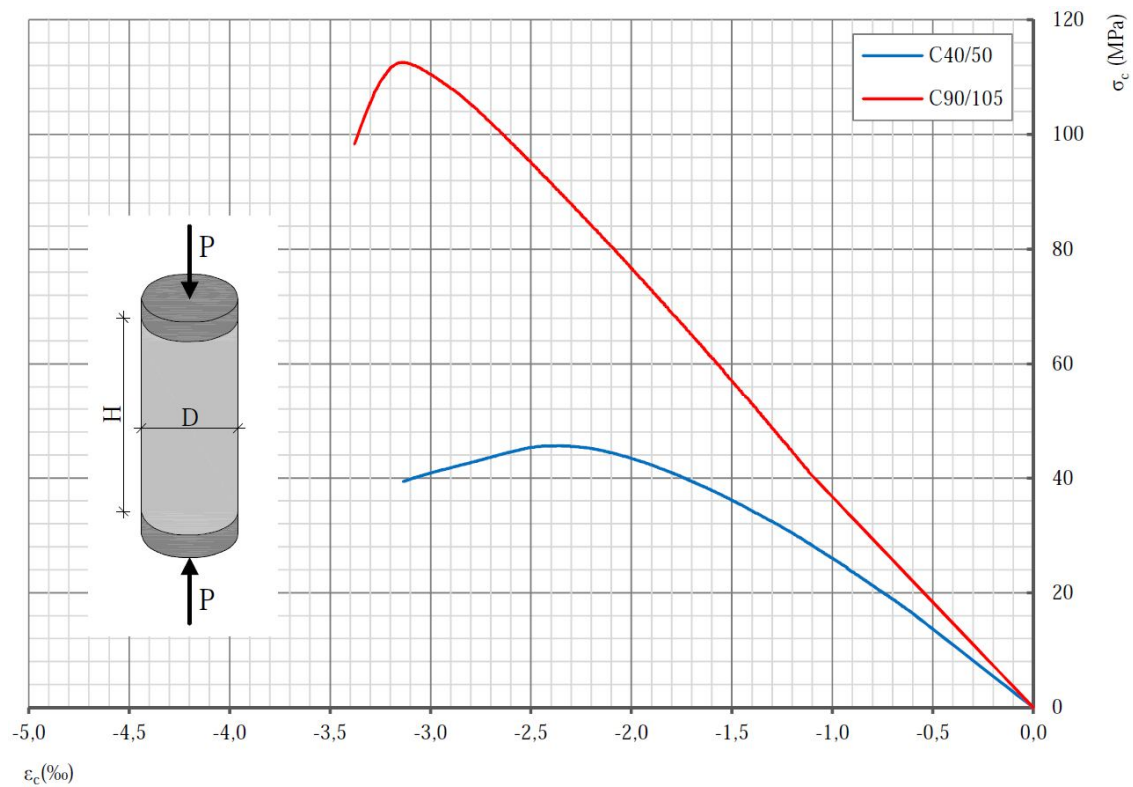Figure 4. Average values of the measured σ_p-ε_p relationship for prestressed steel Y1860S7

Figure 5. Average value of the measured σ_c-ε_c relationship for concrete in compression

The beams were tested under a monotonically increasing static load in the hall where they were made. A rigid steel portal adapted to the needs of the experiment was used. It was concreted into the floor of the hall and had a stiffness sufficient not to become deformed under the loading of the press. The press with a capacity of 500 kN was used, and the maximum stroke of the cylinder is 100 cm. During the test, the beams were supported by massive concrete footings which were additionally secured with diagonal braces. Steel cylindrical bearings were placed on supports to eliminate friction. To avoid horizontal force transfer, cylindrical elements were placed at the point of force input into the beam, with steel plates in contact with the beam to reduce local pressures on the concrete. The following values were measured:

- value of applied force
- deformations of concrete in the lower and upper zone at the midspan
- deformations of selected classic reinforcement profiles in the lower zone at the midspan
- deformations of selected prestressed tendons at the midspan
- deflections of the beam at the midspan
- global behavior of the beam during testing
- crack image of the beam (width, height, spacing and propagation of cracks)

In this paper, the obtained force-displacement diagrams will be used to assess the model behavior. The force applied by the press was divided into two symmetrically distributed forces in relation to the beam center at a distance of 150 cm, so as to obtain pure bending on 150 cm in the central part of the beam.

2. NUMERICAL MODEL

The numerical model for simulating the behavior of the beam is made of member elements. The beam is made as in the experiment, 10 m in length, with a static span of 9.5 m. All five beams are divided into finite elements with an element length of 0.125 m (each beam has a total of 80 elements). [6] The beams are mounted on two movable bearings that simulate cylinders, with a spring of low stiffness (0.01 kN/m) mounted on one bearing to achieve stability in the longitudinal direction of the beam. Both bearings prevent torsional rotation. The sections are made according to the drawings of the actual beams with the exact dimensions of the concrete section and the exact position and amount of classic reinforcement (including shear reinforcement). Three load cases are defined: dead weight, prestressing and force simulating the operation of the press. The dead weight was taken automatically through the known bulk density and volume of the beam. The prestressing was determined so as to match the input data of the experiment, each tendon was modeled separately and a force of 58 kN was applied to each tendon. Two forces of intensity 0.5 kN, located 75 cm away from the beam center on the left and on the right sides so as to satisfy the spacing of 150 cm, were placed on each of the 5 beams as the force simulating the operation of the press. This is equivalent to the load of 1 kN on the press, which is increased by a factor to the numerical failure of the beam. In this case, the load increase factor also shows the actual load at the same time. The beams are shown in Figure 6, and a view of a cross section is shown in Figure 7.
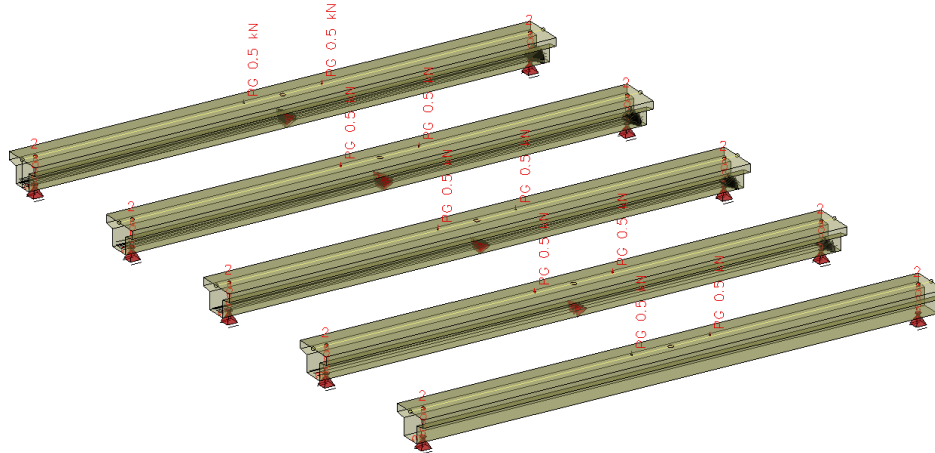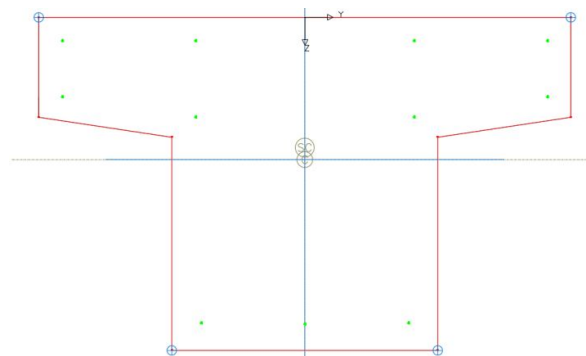

Figure 6. Numerical model of the beams with tendons

Figure 7. Cross section of beam C5

All five beams were analyzed according to the third order theory, and the material nonlinearity was also taken into account in addition to the geometric one. Two material models were used in two calculations for all materials: a design material model according to EC2 rules from which only the fracture values of differently reinforced beams were read and a new material model based on values from the experiment in which a model of concrete behavior in tension was specially made. [3] From the second calculation, force-displacement diagrams were obtained which on the ordinate have the force applied to the beam corresponding to the force on the press from the experiment, and on the abscissa the displacement of a point in the middle of the beam.

Since this is a problem according to the third order theory (large displacement theory), the calculation is performed iteratively. For each increase in load, an equilibrium state is sought by determining new displacements, and stresses based on them, after each iteration. It is checked whether any non-linear effects have occurred on some elements, for example cracks or plasticization. [4] Plasticized elements give different nodal loads compared to linear analysis. These nodal loads of the elements are no longer in balance with the nodal loads of external loads (after the first iteration). The remaining residual forces are set as an additional load in the next iteration. [5] Additional deformations and a new stress state that is generally closer to the equilibrium state are obtained as the result. The maximum residual forces are shown for each iteration. Iterations stop when the residual forces fall below the given tolerance which in this case is relative and is 0.1% of the load for which the beam is checked. The system energy convergence is additionally checked. Energy is proportional to the product of load and displacement. As load is constant, this value represents the global displacement. The ratio of the energy of the current iteration and that of the first (linear) iteration is considered. If this ratio increases, it is a sign that the deformations are still increasing. In this case, even if the residual force satisfies the tolerance, the calculation continues until the system energy reaches a certain convergence. If the energy stops increasing and converges, the deformations are considered to have stopped.

A line search method with a change in tangential stiffness was used to eliminate residual forces in iterations. The load increment decreases depending on the residual forces. If the iteration progresses towards convergence (energy minimum), a new tangential stiffness that improves the behavior of further iterations is generated, if necessary. Cracked elements are taken with reduced stiffness. For better convergence in the fracture zone of the element, the tangential stiffness is adjusted in each iteration. This procedure requires a fairly large number of iterations to converge.

Plastic curvatures are used to determine the nonlinear stiffness. (Figure 8) In this case, the stiffness remains the same and plastic curvatures are calculated; the method is general and generally stable. [7] It also covers biaxial bending and changes in axial stiffness.
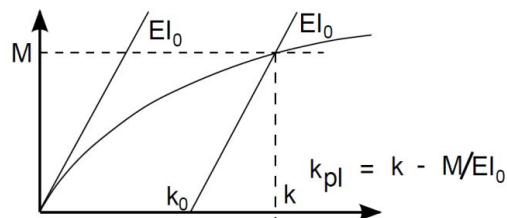

Figure 8. Plastic curvatures

Furthermore, plastic deformations are obtained from given curvatures. In this procedure, the old curvatures are kept and the axial deformations change until the internal and external normal forces are equalized. The internal moments M_y and M_z, which are generally smaller

than the external ones, and the old curvatures give new stiffnesses and plastic curvatures. This method has no problem finding a solution, but requires more iterations. (Figure 9)
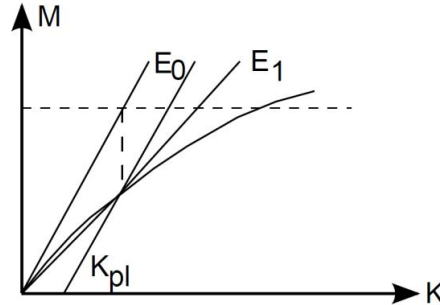

Figure 9. Stiffness determination method

Design and arbitrary models of materials are determined, where the design models are taken from EC2 rules. Arbitrary material models are made according to experimental stress and strain relationships for individual materials, where mean values are taken and models are idealized. Special attention was paid to the modeling of concrete in tension where the peak tensile strength of 7.4 MPa from the experiment was used. The peak tensile strength followed the same slope (same modulus of elasticity) as in pressure and occurs at a deformation of 0.274 ‰. Immediately after that (0.275 ‰), the tensile strength drops to 60% of the value, or to 4.44 MPa. From this value it drops to 0 MPa at a deformation of 2 ‰. For classic reinforcement, a bilinear material model is adopted, where up to the limit of 550 MPa, the reinforcement behaves with a modulus of elasticity of 205 GPa and has a deformation of 2.683 ‰. Subsequently, it progresses to a deformation of 80 ‰ and a stress of 650 MPa. The prestressed reinforcement also has a bilinear material model, it has a modulus of elasticity of 195 GPa up to a stress of 1850 MPa and a deformation of 9.478 ‰. Subsequently, it progresses to a deformation of 60 ‰ and a stress of 2000 MPa. A detailed new material model for concrete is shown below. (Figure 10)

ε[o/oo]	σ-m[MPa]	E-t[N/mm2]
2.000	0.00	-2574
0.275	4.44	-2574
0.274	7.40	-2959977
0.000	0.00	27234
-0.500	-13.50	26532
-1.000	-26.00	22637
-1.500	-36.00	17918
-2.000	-43.50	10691
-2.500	-45.50	-3680
-3.000	-41.00	-10971
-3.140	-39.50	-10586
Safetyfactor		1.50

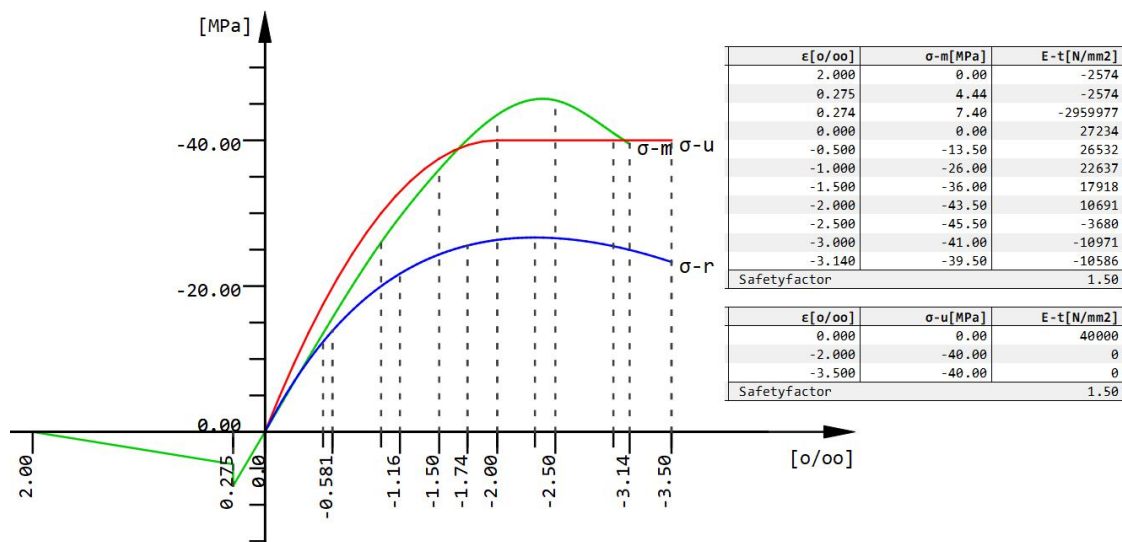| ε[o/oo]	σ-u[MPa]	E-t[N/mm2]
0.000	0.00	40000
-2.000	-40.00	0
-3.500	-40.00	0
Safetyfactor		1.50

Figure 10. Concrete - Design material model (red line)
and arbitrary material model (green line)

3. PRESENTATION AND COMPARISON OF RESULTS

The results of the experiment and of the numerical model, as well as comparisons of the force-displacement diagrams, are presented below. Table 5 shows the experimental results of the force and deflection of the beam center for all beam subtypes. Table 6 shows the results of the force and deflection of the beam center of the numerical model with the design material model according to EC2 (partial safety factor for the material included). Table 7 shows the results of the force and deflection of the beam center of the numerical model with the arbitrary material model (partial safety factor for the material is not included). Figures 11-15 show comparatively the force-displacement diagrams for the beams C1-C5.

Table 5. Experimental results of the force and deflection at the beam center

Results of the type C beam experiment									
C1		C2		C3		C4		C5	
Deflection (mm)	Force (kN)	Deflection (mm)	Force (kN)	Deflection (mm)	Force (kN)	Deflection (mm)	Force (kN)	Deflection (mm)	Force (kN)
0.0	0.0	0.0	0.0	0.0	0.0	0.0	0.0	0.0	0.0
1.5	10.0	1.2	10.0	1.3	10.0	1.8	10.0	2.4	10.0
2.7	20.0	2.4	20.0	2.5	20.0	3.7	20.0	4.2	16.7
4.1	30.0	3.6	30.0	3.7	30.0	5.6	30.0	8.1	20.0
5.4	40.0	4.8	40.0	4.9	40.0	7.6	40.0	13.3	30.0
6.8	50.0	6.0	50.0	6.1	50.0	8.3	42.8	18.1	40.0
8.3	60.0	7.2	60.0	6.7	56.5	11.0	50.0	23.2	50.0
9.9	70.0	8.8	70.0	7.5	60.0	16.9	60.0	27.9	60.0
11.7	80.0	10.7	80.0	10.4	70.0	22.2	70.0	32.7	70.0
13.8	90.0	11.9	84.6	14.9	80.0	27.3	80.0	38.1	80.0
15.7	100.0	13.6	90.0	21.0	90.0	31.8	90.0	43.6	90.0
17.0	105.4	16.7	100.0	27.5	100.0	37.4	100.0	48.0	100.0
19.0	110.0	21.4	110.0	33.6	110.0	43.2	110.0	54.0	110.0
23.2	120.0	26.9	120.0	39.2	120.0	48.5	120.0	60.3	120.0
30.2	130.0	33.4	130.0	47.5	130.0	53.4	130.0	64.0	130.0
38.2	140.0	40.8	140.0	56.2	140.0	59.1	140.0	69.4	140.0
48.0	150.0	50.1	150.0	68.7	150.0	66.3	150.0	88.1	150.0
56.8	160.0	64.0	160.0	127.9	160.0	72.6	160.0	186.1	160.0
93.3	170.0	92.9	170.0	333.5	170.3	101.9	170.0	335.0	170.0
178.7	180.0	178.0	180.0	347.5	170.1	184.4	180.0	453.0	171.1
282.0	183.9	372.0	183.0	372.5	168.3	324.0	182.1	455.2	166.4
288.6	183.4	379.3	177.9	397.5	164.1	332.9	180.1	-	-
-	-	-	-	-	-	339.7	171.7	-	-

Table 6. Results of the force and deflection at the beam center of the numerical model with the design material model according to EC2

Results of the numerical model of the type C beam with the design material model according to EC2									
C1		C2		C3		C4		C5	
Deflection (mm)	Force (kN)	Deflection (mm)	Force (kN)	Deflection (mm)	Force (kN)	Deflection (mm)	Force (kN)	Deflection (mm)	Force (kN)
0.0	0.0	0.0	0.0	0.0	0.0	0.0	0.0	0.0	0.0
0.6	5.0	0.6	5.0	0.6	5.0	1.8	5.0	2.0	5.0
1.2	10.0	1.2	10.0	1.1	10.0	3.9	10.0	4.0	10.0
1.8	15.0	1.7	15.0	1.9	15.0	6.0	15.0	6.1	15.0
2.4	20.0	2.3	20.0	3.2	20.0	8.3	20.0	8.1	20.0
3.0	25.0	2.9	25.0	4.9	25.0	10.6	25.0	10.0	25.0
3.6	30.0	3.4	30.0	7.0	30.0	12.8	30.0	12.1	30.0
4.2	35.0	4.1	35.0	9.3	35.0	15.2	35.0	14.1	35.0
4.7	40.0	4.9	40.0	11.7	40.0	17.6	40.0	16.1	40.0
5.3	45.0	6.1	45.0	14.3	45.0	20.0	45.0	18.2	45.0
6.0	50.0	7.7	50.0	16.9	50.0	22.3	50.0	20.2	50.0
6.8	55.0	9.7	55.0	19.7	55.0	24.8	55.0	22.2	55.0
8.0	60.0	12.1	60.0	22.5	60.0	27.1	60.0	24.3	60.0
9.7	65.0	14.6	65.0	25.2	65.0	29.6	65.0	26.3	65.0
11.6	70.0	17.2	70.0	28.1	70.0	31.9	70.0	28.4	70.0
14.5	75.0	20.3	75.0	30.9	75.0	34.4	75.0	30.4	75.0
17.7	80.0	23.5	80.0	33.9	80.0	37.0	80.0	32.5	80.0
21.2	85.0	26.5	85.0	36.8	85.0	39.4	85.0	34.6	85.0
25.1	90.0	30.0	90.0	39.8	90.0	41.8	90.0	36.5	90.0
29.4	95.0	32.6	95.0	42.9	95.0	44.3	95.0	38.6	95.0
33.6	100.0	36.5	100.0	45.7	100.0	46.7	100.0	40.6	100.0
38.2	105.0	40.1	105.0	48.8	105.0	49.2	105.0	56.0	105.0
43.4	110.0	43.4	110.0	61.9	110.0	56.7	110.0	87.3	110.0
49.2	115.0	47.2	115.0	85.9	115.0	77.9	115.0	131.6	115.0
67.0	120.0	55.5	120.0	137.1	120.0	117.5	120.0	182.5	117.5
101.6	125.0	70.7	125.0	216.8	125.0	199.5	125.0	209.5	118.8
142.8	130.0	107.2	130.0	237.4	125.6	236.6	127.5	204.7	119.2
203.9	135.0	158.4	135.0	-	-	233.5	127.5	-	-
245.9	136.3	207.2	137.5	-	-	-	-	-	-
243.7	136.3	210.6	138.1	-	-	-	-	-	-

Table 7. Results of the force and deflection at the beam center of the numerical model with the arbitrary material model

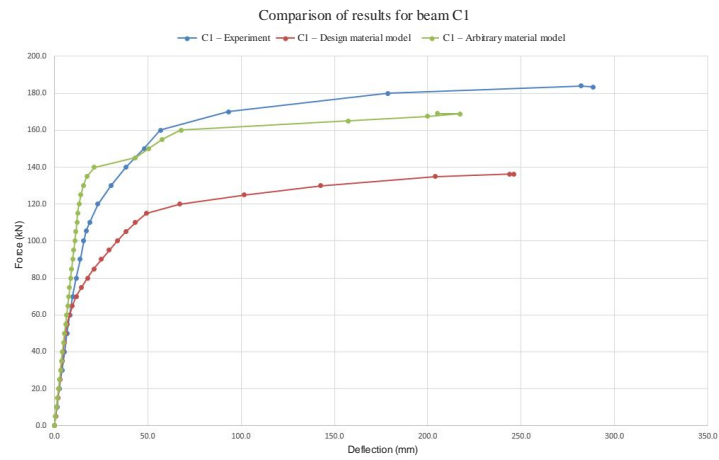| Results of the numerical model of the type C beam with the arbitrary material model									
C1		C2		C3		C4		C5	
Deflection (mm)	Force (kN)	Deflection (mm)	Force (kN)	Deflection (mm)	Force (kN)	Deflection (mm)	Force (kN)	Deflection (mm)	Force (kN)
0.0	0.0	0.0	0.0	0.0	0.0	0.0	0.0	0.0	0.0
0.5	5.0	0.5	5.0	0.5	5.0	0.5	5.0	0.5	5.0
1.1	10.0	1.1	10.0	1.1	10.0	1.0	10.0	1.0	10.0
1.6	15.0	1.6	15.0	1.6	15.0	1.6	15.0	1.5	15.0
2.2	20.0	2.1	20.0	2.1	20.0	2.1	20.0	2.0	20.0
2.7	25.0	2.7	25.0	2.6	25.0	2.6	25.0	2.6	25.0
3.3	30.0	3.2	30.0	3.2	30.0	3.1	30.0	3.1	30.0
3.8	35.0	3.7	35.0	3.7	35.0	3.6	35.0	3.6	35.0
4.4	40.0	4.3	40.0	4.2	40.0	4.2	40.0	4.1	40.0
4.9	45.0	4.8	45.0	4.7	45.0	4.7	45.0	4.6	45.0
5.4	50.0	5.3	50.0	5.3	50.0	5.2	50.0	5.5	50.0
6.0	55.0	5.9	55.0	5.8	55.0	5.7	55.0	6.8	55.0
6.5	60.0	6.4	60.0	6.3	60.0	6.2	60.0	8.4	60.0
7.1	65.0	6.9	65.0	6.9	65.0	6.8	65.0	10.0	65.0
7.6	70.0	7.5	70.0	7.4	70.0	7.3	70.0	11.9	70.0
8.2	75.0	8.0	75.0	7.9	75.0	8.3	75.0	14.1	75.0
8.7	80.0	8.6	80.0	8.4	80.0	9.5	80.0	16.5	80.0
9.3	85.0	9.1	85.0	9.0	85.0	10.9	85.0	19.0	85.0
9.8	90.0	9.6	90.0	9.9	90.0	12.6	90.0	21.7	90.0
10.3	95.0	10.2	95.0	11.0	95.0	14.8	95.0	24.7	95.0
10.9	100.0	10.7	100.0	12.4	100.0	17.3	100.0	27.6	100.0
11.4	105.0	11.2	105.0	14.4	105.0	20.3	105.0	30.2	105.0
12.0	110.0	12.1	110.0	17.0	110.0	23.4	110.0	33.8	110.0
12.5	115.0	13.2	115.0	20.2	115.0	27.2	115.0	36.9	115.0
13.2	120.0	14.6	120.0	24.6	120.0	30.9	120.0	39.9	120.0
14.2	125.0	16.5	125.0	30.4	125.0	34.8	125.0	42.7	125.0
15.5	130.0	19.3	130.0	35.5	130.0	38.5	130.0	45.5	130.0
17.4	135.0	24.3	135.0	40.0	135.0	41.9	135.0	48.3	135.0
21.4	140.0	34.1	140.0	44.2	140.0	45.3	140.0	51.0	140.0
43.4	145.0	39.6	145.0	52.9	145.0	48.5	145.0	182.7	145.0
50.5	150.0	46.0	150.0	63.1	150.0	61.4	150.0	210.2	146.3
57.8	155.0	53.7	155.0	212.8	155.0	180.6	155.0	209.1	146.9
67.8	160.0	60.8	160.0	206.4	155.2	213.0	156.3	-	-
157.4	165.0	72.9	165.0	-	-	221.6	156.9	-	-
199.7	167.5	182.5	170.0	-	-	-	-	-	-
217.2	168.8	221.8	172.5	-	-	-	-	-	-
205.1	169.0	-	-	-	-	-	-	-	-

Figure 11. Comparison of results for beam C1

Figure 12. Comparison of results for beam C2

Figure 13. Comparison of results for beam C3

e-ZBORNIK   21/2021

Jurišić, M., Ćubela, D., Kustura, M.
Simulating the behavior of prestressed beams with different degrees of prestressing
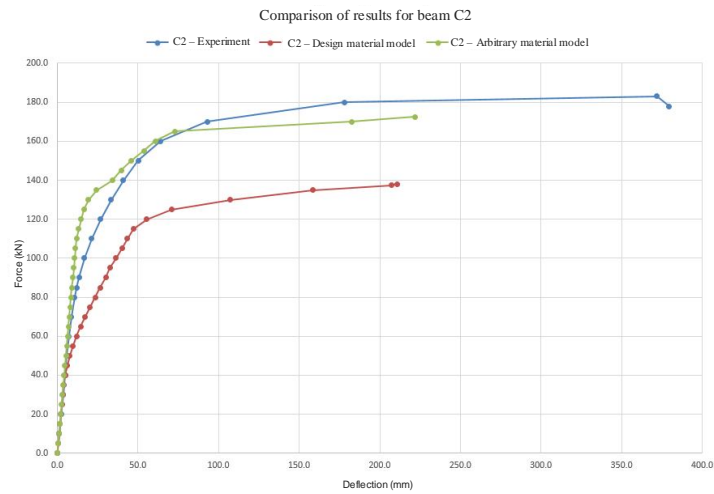
Figure 14. Comparison of results for beam C4
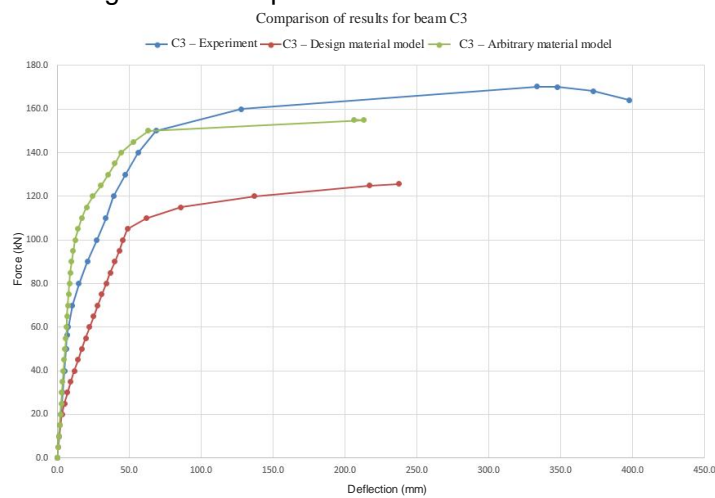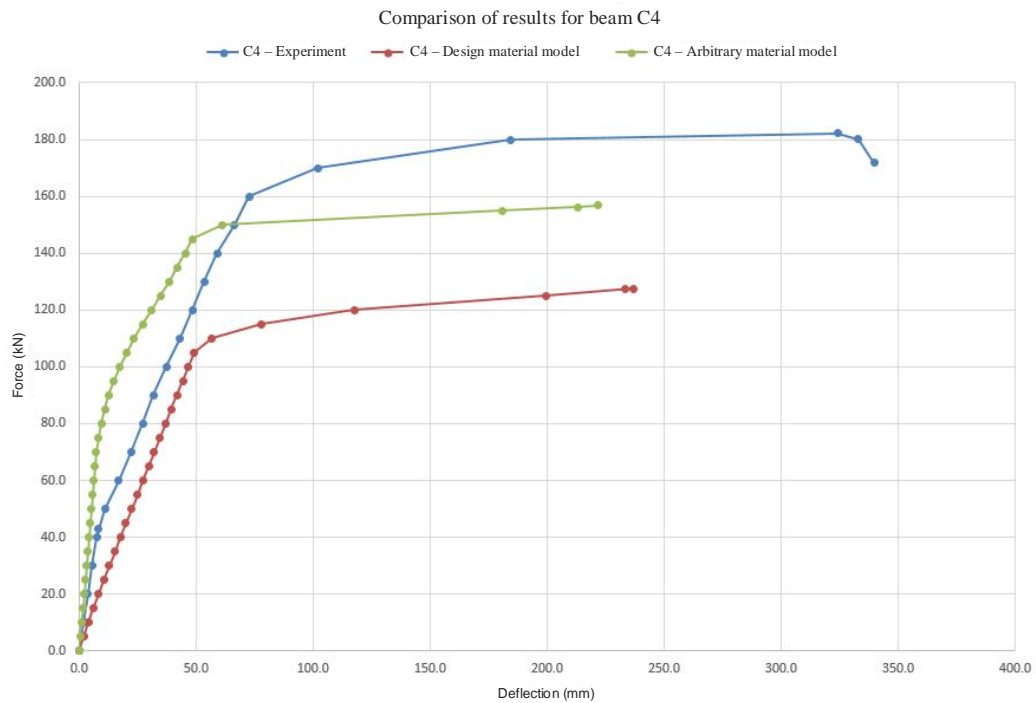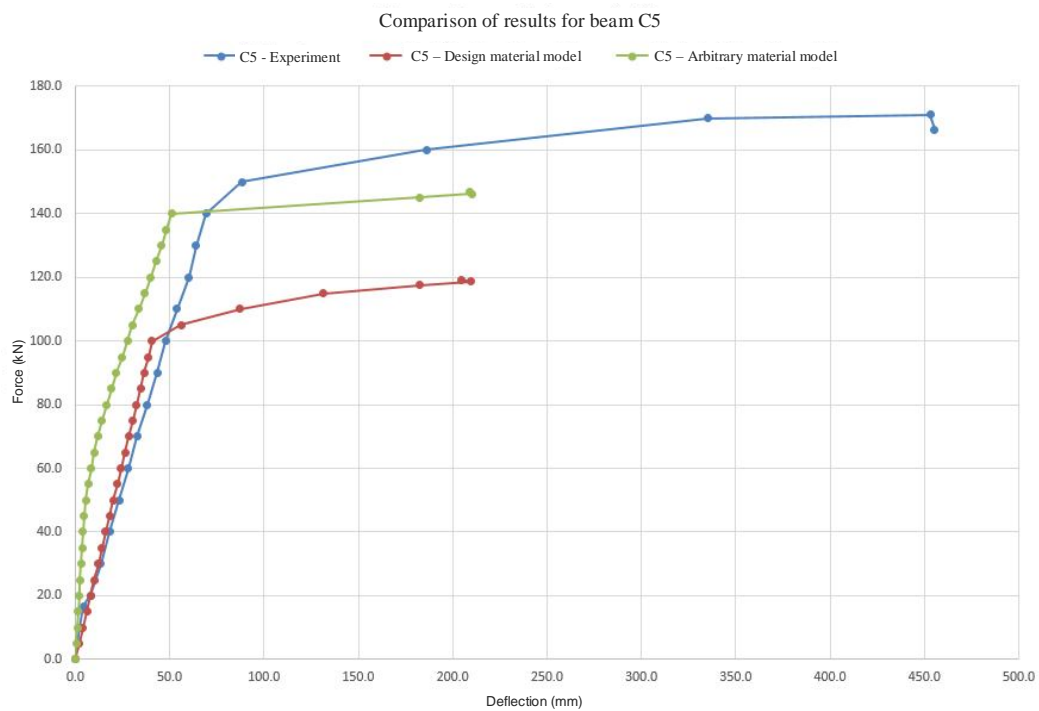

Figure 15. Comparison of results for beam C5

4.   CONCLUSION

It can be observed that the designed beam failure force is roughly equal for all beams and ranges from 119.2 kN for beam C5 to 138.1 kN for beam C2. The mean value of the design failure force is 129.34 kN and the maximum deviation is 8%. The reason for the deviation is the impossibility of the exact ratio of classic to prestressed reinforcement due to the available surfaces of tendons and bars. The mean failure force of the beam in the experiment is 178.08 kN with a maximum deviation of 3%. The mean failure force of the beam with the arbitrary material model is 160.08 kN with a maximum deviation of 8%. The maximum difference between the failure force of the experiment and the failure force with the arbitrary material model is on beam C4 and is 25.2 kN, which is a deviation of 14%. The minimum difference is on beam C2 and is 10.5 kN, which is a deviation of 6%. Considering that concrete is not a homogeneous material and that data tested on part of the elements were included in the arbitrary material model, it can be concluded that the failure values of the numerical model coincide well with the actual failure values. Regarding the displacements, it can be concluded that the displacements achieved in all experimental force-displacement diagrams were larger than in the numerical ones. The reason for this is that it is very difficult to achieve numerical convergence near the failure limit, because the stress and strain state changes significantly for a small load increment due to the large decrease in stiffness.

It is most important to compare the global behavior of the beams. It is evident that the linearity limit (until the opening of the first crack) in the experiment and even in the numerical model decreases as the degree of prestressing decreases. On all beams, it is observed that the linearity limit in the numerical model is greater than in the experiment by 30 kN on average. The most likely reason is the tensile strength of concrete. The tensile strength of concrete C40/50 of 7.4 MPa was shown in the experiment, which is significantly greater than the usual average tensile strength of 3.5 MPa. The tensile strength of concrete has a great effect on the linearity limit, i.e. the greater it is, the greater the linearity limit is. According to this, there is a possibility that the actual tensile strength was closer to the value of 3.5 MPa on the beams in the experiment, as opposed to the samples. After the linearity limit, the diagram branches are almost parallel, which means that the beams in the numerical model behave very similarly to the actual beams, and that arbitrary material models describe well the behavior of the materials.

REFERENCES

1. Ćubela, D.: Usability properties of concrete structures depending on the degree of prestressing, doctoral thesis, Faculty of Civil Engineering, University of Mostar, Mostar, 2017.
2. Markić, R.: Influence of relation of prestressed and classical reinforcement on the behavior of concrete beam structures, doctoral thesis, Faculty of Civil Engineering, Architecture and Geodesy, University of Split, Split, 2012.
3. EN 1992-1-1 (2004): Eurocode 2: Design of concrete structures – Part 1-1: General rules and rules for buildings, 2004.
4. Petronijević, M.: Teorija konstrukcija 1, Univerzitet u Beogradu – Građevinski fakultet, Akademska misao, 2019.
5. Fertis, D.G.: Nonlinear Structural Engineering, Springer, 2006.
6. Harapin, A., Trogrlić, B.: Uvod u metodu konačnih elemenata – Štapni sustavi u ravnini (Introduction to the finite element method - In-plane beam systems), Internal course materials, University of Split, Split, 2009.
7. Ghaboussi, J., Pecknold, D.A., Wu, X.S.: Nonlinear Computational Solid Mechanics, CRC Press, 2017.